Heliyon 10 (2024) e28666

Contents lists available at ScienceDirect

Heliyon

journal homepage: www.cell.com/heliyon

Research article

Chitosan nanoparticle and its effect on *Neoscytalidium novaehollandiae*, the causal agent of mulberry canker in Tehran

Naemeh Mohammadi [a], Naser Safaie [a,*], Maryam Nikkhah [b], Sajad Moradi [c]

[a] Department of Plant Pathology, Faculty of Agriculture, Tarbiat Modares University, Tehran, Iran
[b] Department of Nanobiotechnology, Faculty of Biological Sciences, Tarbiat Modares University, Tehran, Iran
[c] Nano Drug Delivery Research Center, Health Technology Institute, Kermanshah University of Medical Sciences, Kermanshah, Iran

ARTICLE INFO

Keywords:
Biopolymer
Landscape trees
Nano fungicide
Nanomaterial

ABSTRACT

Fungal pathogen "*Neoscytalidium novaehollandiae*" is the causal agent of trunk canker in mulberry trees. Mulberry is considered as most valuable tree for landscaping in Tehran. Here in, for the first time, chitosan nanoparticles (CSNPs) were used to inhibit canker disease causal agent of mulberry. For this purpose, CSNPs were synthesized with a yield of 86%, and after characterization of the synthesized nanoparticles, the growth inhibition rate of fungus (GI%) was evaluated. The results of *in vitro* assays showed that the concentration of 1500 ppm significantly ($P \leq 0.05$) decreased the radial growth of the fungus in comparison with control. For *in vivo* experiments, 2-year-old branches from healthy randomly selected mulberry trees in the landscape, were inoculated artificially in the laboratory with mycelial plugs from a 7-day-old culture of fungus. The infected branches were then treated with 500, 1000, and 1500 ppm of CSNPs. The results indicated that the disease severity (DS%) in all the treatments and the control plants increased over time. However, the slope of the changes in DS was less in CSNPs treated compared to control. This effect was concentration dependent so that no disease progress was observed at 1500 ppm of CSNPs. The findings indicate the effectiveness of CSNPs in control of canker disease of mulberry caused by *N. novaehollandiae*.

1. Introduction

Mulberry trees (*Morus* sp.) with low water requirements, and resistance to pruning, wind, drought, and pollution are very suitable plants for urban conditions, home gardens, shading streets, and beautifying cities. Mulberry is a perennial, fast-growing, deciduous plant of the *Moraceae* family, which includes various species commonly known as mulberries [1].

The genus *Neoscytalidium*, which is related to canker and blight on a wide range of fruit and forest trees such as mulberry trees [5], belongs to *Botryosphaeriaceae* family with six species i.e., *N. dimidiatum*, *N. hyalinum*, *N. novaehollandiae, N. orchidacearum* [2], *N. oculus* [3], and *Neoscytalidium hylocereum* sp. nov [4].

In recent years, *N. novaehollandiae*, described by Palvic et al. [5], has been reported as one of the most important species from various hosts, such as mango (*Mangifera indica*) [6], Persian oak (*Quercus brantii*) [7], pistachio (*Pistacia vera*) [8], grapes (*Vitis vinifera*) [9], tomato (*Solanum lycopersicum*) [10], Japanese persimmon (*Diospyros kaki*) [11], almonds (*Prunus dulcis*) [12,13], pears (*Pyrus*

* Corresponding author.
E-mail address: nsafaie@modares.ac.ir (N. Safaie).

https://doi.org/10.1016/j.heliyon.2024.e28666
Received 10 December 2023; Received in revised form 20 March 2024; Accepted 21 March 2024
Available online 26 March 2024

communis) [14], sage (*Salvia officinalis*) [15], mulberry (*Morus alba*) [5], cherry tree (*Prunus avium*) [16], plum (*Prunus domestica*) [17], and pine (*Pinus eldarica*) [3].

Currently, *N. novaehollandiae* is the dieback causal agent of pine trees, as the most common urban trees in Tehran. This pathogen can survive in coniferous fruits dropped at the foot of the trees and by production high population of air-born black powdery spores under torn skin can infect other injured or weakened hosts like mulberries [3].

Recently, in the field observations this species appeared in mulberry trees in the Tehran landscape with symptoms like drying branches, branch canker, and dieback with internal vascular discoloration [5].

Considering the importance of mulberry trees in the urban environment and the possibility of dissemination with air-borne spores of *N. novaehollandiae*, this study was conducted to find a way to inhibit the fungus on important trees in Tehran including mulberries.

The most common method for the management of canker disease caused by *Neoscytalidium* spp. is the application of synthetic chemical fungicides [18–20].

Since no information is available about the synthetic fungicides for the management of *N. novaehollandiae* as the topic discussed, and also due to close relationship of this species with *N. dimidiatum* [21], the focus was only on research related to chemical control of *N. dimidiatum* in this study.

Active ingredients from different chemical groups with the strong inhibitory effect on *N. dimidiatum* include Demethylation Inhibitor Group (DMI, triazole)-difenoconazole, tebuconazole, hexaconazole, cyproconazole, triadimefon-; EoI Group (Strobilurins) -azoxystrobin; and Dicarboximide Group-iprodione [22]. It was reported that the mycelial growth *of N. dimidiatum*, the causal agent of dragon fruit (*Hylocereus undatus*) stem canker disease, was effectively controlled by cyprodinil + fludioxonil, azoxystrobin + difenoconazole, and tebuconazole, also spore germination was controlled by metiram, trifloxystrobin, pyraclostrobin, azoxystrobin, azoxystrobin + difenoconazole and iminoctadine [23]. It was describe that *N. dimidiatum*, causing the sooty canker of Eucalyptus (*Eucalyptus camaldulensis*) branches, inhibited by the fungicide Beltanol-L (1 ml/L) and salicylic acid (1 g/L) [24]. The growth of *N. dimidiatum*, the causal agent of stem canker in dragon fruit (*Hylocereus undatus*), inhibited completely in PDA medium amended with manganese ethylenebis (5 mg/ml) and pyraclobin (2.5 ml/L). Isoprothiolane (62 ml/L) also brought promising results (100% inhibition of fungal growth) [25].

Although synthetic fungicides have definite and quick effects on plant pathogens, they can be dangerous for human health and the environment [26]. The development of the application of nanoparticles in plant pathology has led to the use of antimicrobial nanomaterials over the last decades [27] and the potential applications of nanoparticles/materials as antifungal agents have also been investigated. Among the nanomaterials with antimicrobial properties, CSNPs as a natural material with excellent physicochemical, antimicrobial, and biological properties, have absorbed great attention due to their high permeability, biodegradability, non-toxicity for humans and the environment, as well as cost-effectiveness [28]. According to Kheiri et al. [28], under *in vitro* conditions, CSNPs at concentrations of 500 ppm and 900 ppm inhibited the growth of *Fusarium graminearum* by 31.97% and 29.67%, respectively. The antifungal effects of CSNPs on the other plant pathogenic fungi including inhibition the mycelial growth of *Pyricularia grisea* by 65% and *Macrophomana phaseolina* by 84% at 1000 ppm, *Colletotrichum gloeosporioides* by 85.7%, *Phytophthora capsica* by 50.7%, *Sclerotinia sclerotiorum* by 39.5%, *Fusarium oxysporum* by 50.3% and *Gibberella fujikouri* by 56.3% at 5000 ppm. CSNPs also inhibited the growth of *Alternaria alternate* by 80.1–82.2% and *Rhizoctonai solani* by 32.2–34.4% at 600–1000 ppm, and *A. solani* by 62.75% at 300–400 ppm. Moreover, *Alternata tenuis*, *Aspergillus niger*, *A. terreus*, *Baeuvaria bassiana*, *F. graminearum*, *F. oxysporum*, *Sclerotium rolfssi* growth were inhibited by 67.67%, 62.75%, 74.67%, 70.08%, 60.37%, 66.66%, and 43.7%, respectively using 800 ppm CSNPs [29].

For evaluation of the management strategies such as the use of fungicides, disease should be quantified to determine its temporal and spatial dynamics [30]. One of the ways to quantify the disease is calculation of the disease severity, which is usually evaluated by the visual symptoms of the disease [31]. In the case of fungi such as *Neoscytalidium* that cause lesions on the plant, the severity of the disease can be evaluated by measuring lesion diameter [3].

Recently, the antifungal effects of nanoparticles Cu_2–*O*–Cu stabilized with alginate and chitosan-silver nanoparticles, as a nano delivery system, in combination with the Zinc Ethylene Bisdithiocarbamate fungicide, against the *N. dimidiatum*, the causal agent of the brown spot disease of dragon fruit, was confirmed in laboratory condition [32].

So far, there has been no study on the antifungal effect of CSNPs on *N. novaehollandiae*. Therefore, CSNPs were used in this study to control *N. novaehollandiae* which causes canker disease in mulberry trees.

Also, the logistic model was used to analyze the effect of synthesized CSNPs on the *N. novaehollandiae*, the causal agent of mulberry canker.

2. Materials and methods

Low Molecular Weight (LMW) chitosan with CAS number: 9012-76-4 (Mw: 50–190 kDa; degree deacetylation: 75–85 %) was purchased from Sigma-Aldrich (Germany). The Captan fungicide powder (Agrow Allied Ventures Pvt. Ltd., India) as the positive control in the bioassays, were donated by Melli Shimi Keshavarz Company (Tehran, Iran). Pure culture of *N. novaehollandiae*, the causal agent of canker disease in mulberries, was obtained from the Laboratory of Plant Diseases Management, Department of Plant Pathology, Faculty of Agriculture, Tarbiat Modares University, Tehran, Iran.

2.1. Synthesis and characterization of CSNPs

Among the various procedures for the synthesis of CSNPs, the ionic gelation method is the most widely used one. This method, first reported by Calvo et al. [33], is based on the electrostatic interactions between the amino groups of chitosan and the negatively

charged groups of a polyanion such as tripolyphosphate [29]. In this study, CSNPs were prepared based on the ionic gelation method according to Kheiri et al. [28].

To measure the size and surface charge of CSNPs, the hydrodynamic size and zeta potential of the nanoparticles were determined by a dynamic light scattering (DLS) analyzer (Malvern NanoZS, beam: 2000–3500 KCPS, UK) [28]. Scanning electron microscopy (SEM) was used to study the surface morphology of CSNPs [34] using a MIRA3 TESCAN microscope at 10 kV. Fourier transform infrared (FTIR) spectroscopy (ThermoScientific-NicoletIR100, KBr pellet, China) was used for confirming the synthesis CSNPs and determination of the functional groups [34]. Also, Eq. (1) was used to calculate the yield percentage of CSNPs synthesis [28]:

$$Yield\ (\%) = (W_r / W_s) \times 100 \quad (1)$$

Where W_r is dry weight of the recovered nanoparticles, and W_s signifies the sum of initial dry weight of starting material.

Furthermore, to evaluate the colloidal stability of the CSNPs, samples were stored at ambient temperature for sixty days, then the size and zeta potential of nanoparticles were measured using a DLS analyzer at different time points [35].

2.2. Evaluation of CSNPs inhibition effects on N. novaehollandiae

2.2.1. In vitro assay

The concentrations of CSNPs used for the control of most of the plant pathogenic fungi in recent researches were extracted and optimized for conducting *in vitro* experiments. To evaluate the inhibitory effect of CSNPs on radial growth of *N. novaehollandiae*, potato dextrose agar (PDA) medium was amended with 100, 250, 500, 1000, 1500, and 2000 ppm of CSNPs and poured into Petri dishes in triplicate. Then, a fungal disk of 7-day fungal culture medium with a diameter of 5 mm was placed in the center of each Petri dish [28]. As a positive control, Captan fungicide at a concentration of 1500 ppm was used, and buffer with pH = 5 was used as a negative control. The inoculated petri dishes were incubated at 28 °C and in the dark, and after 7 days the radial growth of the fungus was checked. These tests were repeated 2 times and the percentage inhibition rate of fungal growth was calculated using Eq. (2) [28]:

$$Growth\ Inhibition\ Rate\ (\%) = [(R_c - R_t) / R_c] \times 100 \quad (2)$$

Where R_c is radial mycelial growth in control plate, and R_t signifies radial mycelial growth in CSNPs treated plates.

2.2.2. In vivo assay

In vivo assay was conducted according to the previous studies [3,36–38] with modifications. The 2-year-old branches with 2 cm diameter from healthy randomly selected mulberry trees were chosen and cut into 20 cm long pieces. A total of 52 fresh and healthy branches (36 pieces for pathogenicity tests, 15 pieces as a negative control including PDA, buffer and concentrations of 500, 1000, and 1500 ppm of CSNPs, and 1 piece as a positive control) were used for *in vivo* pathogenicity tests. After disinfecting their surfaces with 72% ethanol and removing a part of the skin and a slight part of the wood in the middle of the cut branches, they were treated with one drop (equivalent to 50 μL) of buffer, 500, 1000, and 1500 ppm of CSNPs named C1, C2, C3, and C4, respectively in 9 replicates (3 replicates for each treatment × 3 replicates for three sampling days i.e. 14 days, 28 days, and 42 days after inoculation) and then inoculated with a 5 mm diameter fungal disc from 7-day-old fungal culture. For the positive control, 1500 ppm of aqueous solution of Captan (10 mg/ml) was used as a positive control in pathogenicity experiments. The negative control samples were also inoculated with a PDA disk (named C0 treatment). All of the inoculated branches were sealed with Parafilm, and both ends of them were also covered with wet cotton to prevent the removal of moisture from the cutting branches and incubated in the growth chamber at 27 °C for 42 days and checked every 14 days. Before performing *in vitro* and *in vivo* tests, Koch's postulates were performed to corroborate the pathogenicity of the fungus.

To quantify the results of *in vivo* test, disease severity (DS%) was calculated by Eq. (3) [3]:

$$Disease\ Severity\ (\%) = [(LL / BL)] \times 100 \quad (3)$$

Where LL is the lesion length, and BL is the length of the branch. The length of the branch in all samples is the same and equal to 20 cm.

Also, the logistic model Eq. (4) was used to calculate the disease progress in the mulberry branches inoculated with *N. novaehollandiae* and control ones treated with three concentrations of CSNPs (500, 1000, and 1500 ppm) and to investigate the antifungal effects of CSNPs over time.

$$Logit\ (Y_t) = r_L t + C \quad (4)$$

Where Y_t is disease severity, t is time in days, r_L is logistic infection rate and C is proportionality constant.

The infection rate of disease in logistic model (r_L) was also calculated and the linear regression equation presented.

2.3. Statistical Analyses

The experiments were performed with three replications and based on a Completely Randomized Design (CRD). Statistical analysis, and comparison of means using Duncan's multiple range test were done using SPSS 20.0 software.

3. Results

3.1. CSNPs characterization

Calculation of synthesis yield of CSNPs showed that, 86% of the all starting materials converted into nanoparticles. The average hydrodynamic radius of the synthesized CSNPs in three repeats was 200.1 ± 15.5 nm with the polydispersity index (PDI) of 0.17 indicated a narrow particle size distribution. Also, the average value of zeta potential was +27.46 ± 1.35 mV. The hydrodynamic radius and zeta potential of prepared CSNPs from one of the three repeats is shown in Fig. 1 (a, b). Moreover, the data obtained from CSNPs colloidal stability test within 60 days, indicated high stability of nanoparticles and no significant differences were observed in particle size and particle size distribution over time (Table 1S). Scanning electron microscope was used to study the morphological characteristics of CSNPs. Images demonstrated the spherical shape of nanoparticles with a size distribution in the range of 30–50 nm and uniformity of synthesized CSNPs (Fig. 1 (c)). The functional groups of CSNPs were investigated by FTIR spectroscopy confirming the CSNPs formation. The infrared absorption spectrum of CSNPs and their components namely chitosan and tripolyphosphate are presented in Fig. 1 (d). In the case of chitosan, there are 3 specific peaks in the ranges of 1380, 1470, and 1620 cm^{-1}, which are related to CH and OH bending, N–O stretching and amine bending, respectively. The characteristic peak of P═O stretching can be seen in the 1150 cm^{-1} region of the tripolyphosphate spectrum [39].

3.2. In vitro bioassay

The antifungal activity of CSNPs (100, 250, 500, 1000, 1500, and 2000 ppm) against *N. novaehollandiae* enhanced with increasing the concentration of nanoparticles. Among them, the concentration of 1500 ppm (with %GI = 100) displayed the maximum growth inhibition and showed significant effect compared with control [Fig. 2(a–h), Table 1]. So, the concentration of 1500 ppm was reported as minimum inhibition concentration (Table 1). Also, no significant difference in fungal growth was observed between 100 ppm CSNPs and control (Table 1).

3.3. In vivo bioassay

The length of lesions and branch canker symptoms created by *N. novaehollandiae* decreased with nanoparticle treatments especially at a concentration of 1500 ppm in the first and second sampling days [Fig. 3 (a-r)], indicating the effectiveness of CSNPs in controlling the canker disease and stopping the progress of the pathogen in the mulberry tree branches as a host tissue. In addition, being symptomless of the negative control samples including PDA, buffer and concentrations of 500, 1000, and 1500 ppm of CSNPs indicated

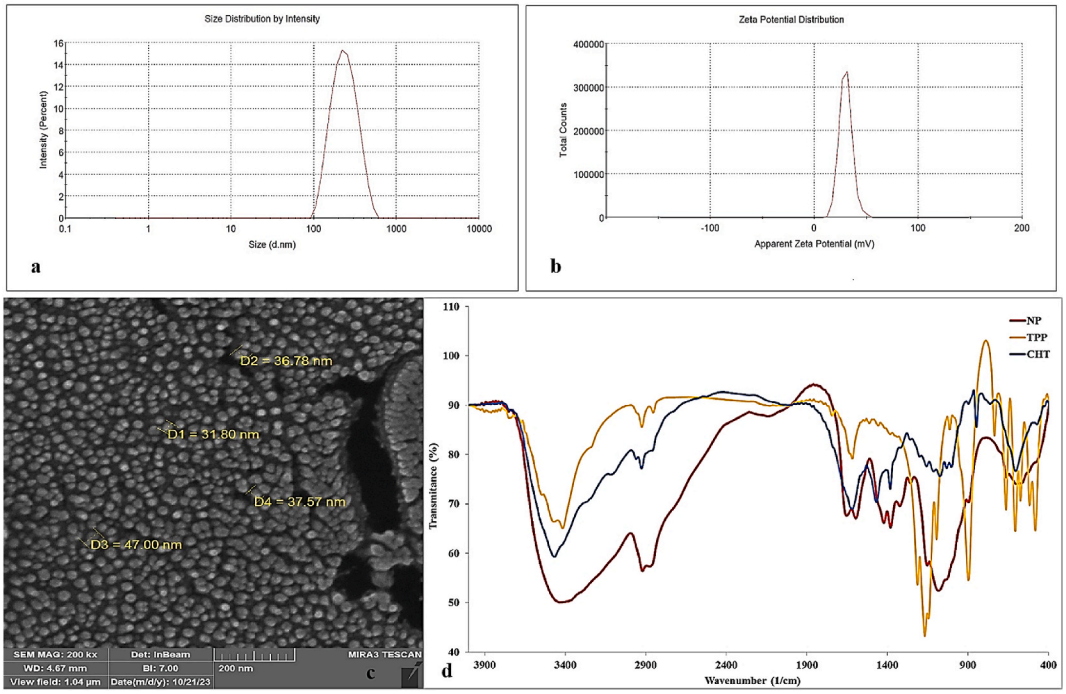

Fig. 1. Chitosan nanoparticles (CSNPs) characterizations results; (a) CSNPs size is 219.8 nm with PDI = 0.17. (b) CSNPs zeta potential is +30.1 mV. (c) Scanning Electron Microscope (SEM) image of CSNPs. (d) Fourier transform infrared (FTIR) spectrum of Chitosan nanoparticle (NP), Chitosan biopolymer (CHT) and Tripolyphosphate (TPP).

Table 1
Effects of different concentrations of chitosan nanoparticles (CSNPs) on radial growth and growth inhibition rate of *N. novaehollandiae*.

CSNPs Concentrations (ppm)	Repeat	Radial Growth	Growth Inhibition Rate (%)
Control	3	6.33[a]	0
100	3	5.88[ab]	7.1
250	3	5.45[b]	13.9
500	3	4.43[c]	30.01
1000	3	2.31[d]	60.34
1500	3	0[e]	100
2000	3	0[e]	100

Means with the same letter are not significantly different.

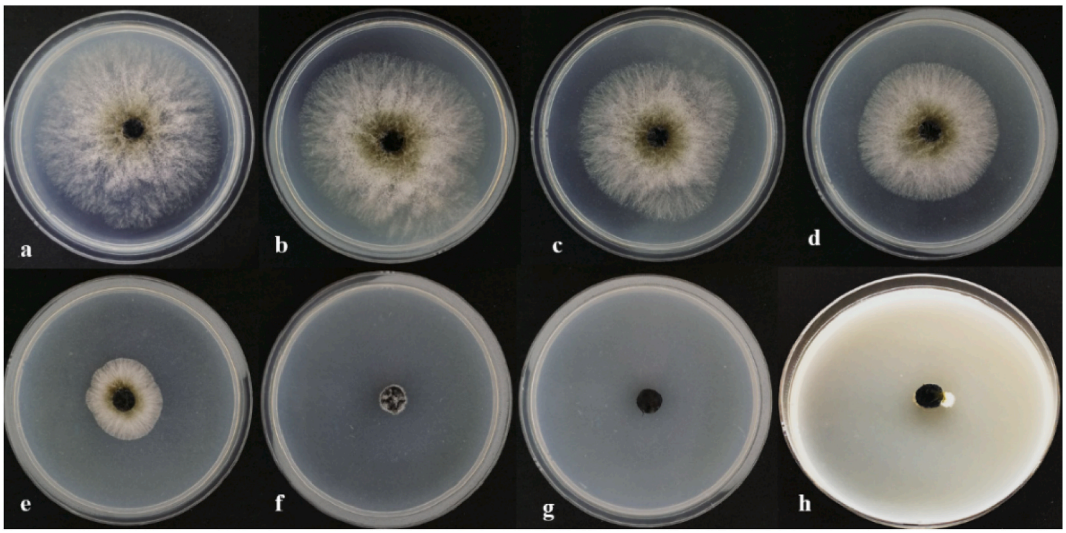

Fig. 2. Effect of different concentrations of CSNPs (a: negative control, b: 100 ppm, c:250 ppm, d: 500 ppm, e: 1000 ppm, f: 1500 ppm, g: 2000 ppm, and h: positive control/1500 ppm of Captan) on radius mycelial growth of *N. novaehollandiae*.

that none of them caused lesions in the mulberry branch tissue and the branch canker only was due to the inoculation of the branches with the fungal culture [Fig. 3 (m-r)].

Based on the results of profile plot (Fig. 4), the disease severity of all three treatments (500, 1000, and 1500 ppm) and the control increased during time. However, the highest disease severity was related to the control at three sampling days, especially at the third sampling day (33.33%; Fig. 4) and the lowest disease severity was recorded in 1500 ppm of nanoparticles at three sampling days especially at the first and second sampling day (11.33%; Fig. 4). In general, adding CSNPs with any concentration in all three sampling days reduced the disease severity compared with control. The disease severity in all concentrations and also in the control had an upward trend from the first sampling day to the third one. However, the slope of the changes from the first to the third sampling day and the upward trend in the treatments decreased with increasing the concentration of nanoparticles. So the branches treated with 1500 ppm of CSNPs reduced the disease progression and was close to zero (Fig. 4).

According to the statistical analysis, the main effects of sampling days and concentration of CSNPs and their interaction effects on disease severity were significant (table 2S). Also, different sampling days influenced disease severity. The eta squared coefficient also showed that different concentrations of CSNPs, sampling days, and the interaction of concentration and sampling days had an effect of 93%, 65%, and 59%, respectively on the disease severity. Also, the statistical power related to the concentration of nanoparticles, sampling days, and sampling days *concentration was 1, 1, and 0.98, respectively. The reported values were more than 0.7, which indicated the appropriateness of the number of samples to investigate the effect of the mentioned variables on the disease severity. The coefficient of determination of the test showed that concentration and sampling days could explain 95% of the changes in the disease severity (table 2S).

The disease progress curve of mulberry branches test in control and 500, 1000, and 1500 ppm of CSNPs showed that the slope of changes from day 14 to day 28 after inoculation was constant, but the distance between the graphs from the control to the CSNPs treatment (500, 1000, and 1500 ppm) displayed that the disease severity from 14th day to 28th day after inoculation in the control was more than that in other treatments, and the lowest of it recorded at 1500 ppm. On the other hand, from 28th day to 42nd day after inoculation, the upward trend of control was almost similar to 500 ppm treatment. In the graph of 1000 ppm nanoparticles, the slope of the ascending line was milder compared with the control and 500 ppm treatment, and the lowest slope of the line in this period was related to 1500 ppm nanoparticles. The disease severity was constant from 14th day to 28th day, and also 28th to 42nd day after inoculation, it was very slow and close to zero (Fig. 5).

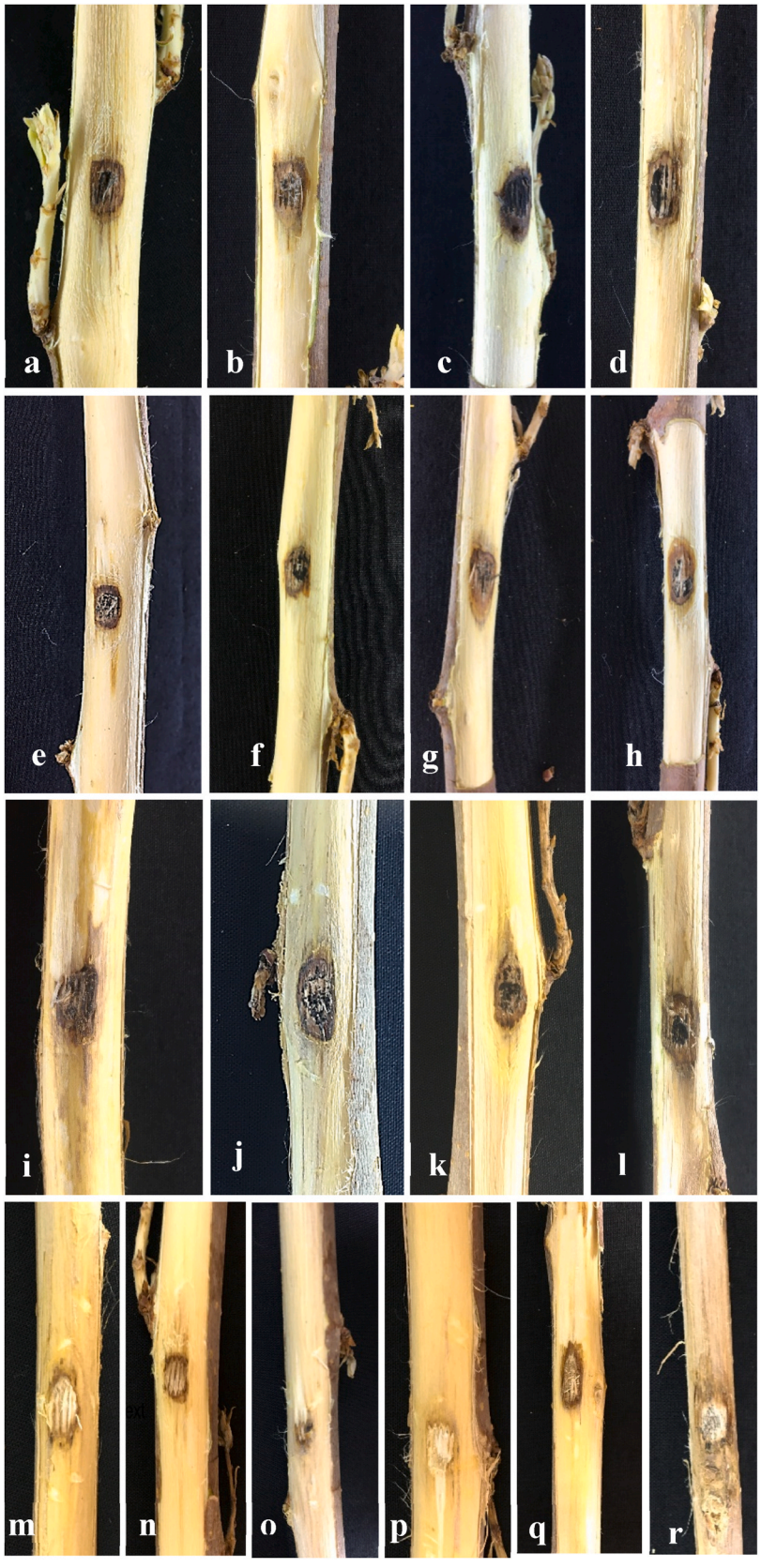

(caption on next page)

Fig. 3. Pathogenicity tests on mulberry branches. Images from a to l are related to treatments (a:T1C1, b: T1C2, c: T1C3, d: T1C4, e: T2C1, f: T2C2, g: T2C3, h: T2C4, i: T3C1, j: T3C2, k: T3C3, l: T3C4) and from m to q are related to negative controls (m: C0, n: C1, o: C2, p: C3, q: C4) and image r is positive control. T1, T2, and T3 represented first sampling day (14 day after inoculation), second sampling day (28 day after inoculation), and third sampling day (42 days after inoculation) respectively. C0, C1, C2, C3, C4 represented PDA, buffer (pH = 5), 500, 1000, and 2000 ppm of CSNPs concentration, respectively. As it can be seen negative controls are symptomless (below) and the length of lesions created by the pathogen had decreased with nanoparticle treatments especially at a concentration 1500 ppm in the first and second sampling days (d, h).

The linear regression diagram showed that the disease rate changes from the control to 500, 1000, and 1500 ppm treatments had a downward trend (Fig. 6).

4. Discussion

As mentioned in previous studies, CSNPs show stronger antifungal activity compared with bulk chitosan which is probably due to the higher density of surface to charge, more surface area and better absorption of CSNPs by fungal cells [40].

Characterization of synthesized CSNPs is crucial for better understanding the nanoparticle formation mechanism and also physicochemical and antifungal properties of CSNPs [41]. All of the characterization techniques conducted in this study confirmed the formation of stable CSNPs with uniform small size and high positive surface charge by interacting primary bulk chitosan sample with TPP in ionic gelation method. Among the CSNPs characterization results, the FTIR results demonstrated the bands relating to functional groups of both the chitosan and polyphosphate. However, as in previous studies, the broadening and separation of the peaks in all parts were seen, which could be due to the interactions between the components [32]. Therefore, it was assumed that poly

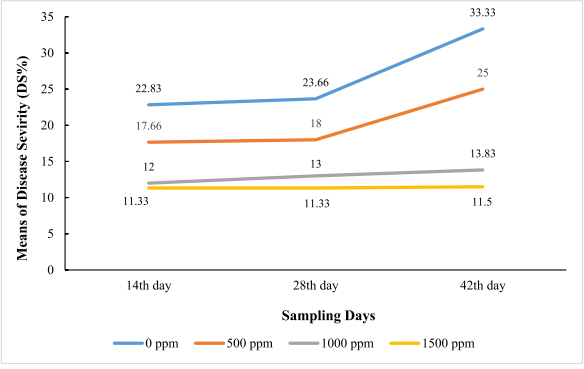

Fig. 4. The plot related to the highest and lowest severity of the canker disease caused by *N. novaehollandiae* over time after treatment of the infected mulberry branches with 500, 1000, and 1500 ppm concentrations of CSNPs.

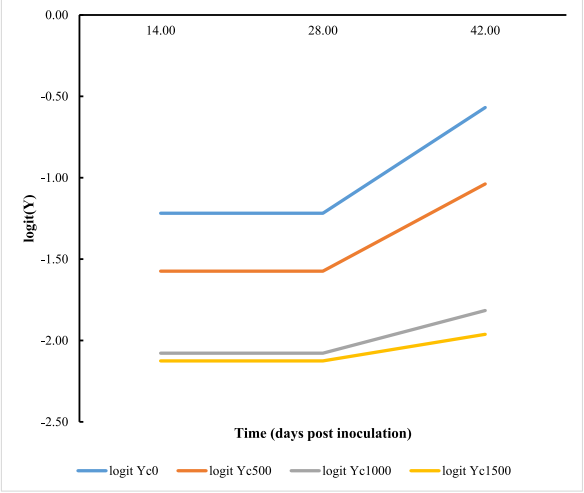

Fig. 5. Canker disease progress curve over time. Canker disease progress in the inoculated mulberry branches with *N. novaehollandiae* and control sample which were treated with three concentrations of CSNPs (500, 1000, and 1500 ppm). At concentration 1500 ppm the disease progress curve is very slow and close to zero that suggested that the disease was inhibited at this treatment.

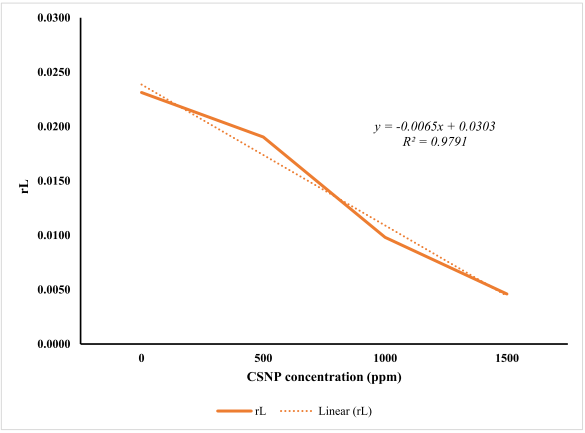

Fig. 6. Logistic infection rate. Infection rate of *N. novaehollandiae* in the inoculated mulberry branches with *N. novaehollandiae* and control sample which were treated with three concentrations of CSNPs (500, 1000, and 1500 ppm). The rate of disease changes from the control to the 500,1000, and 1500 ppm treatments has a downward trend.

phosphoric groups in sodium polyphosphate interacted with the ammonium groups of chitosan, contributing to an increase in both inter- and intramolecular interaction in CSNPs.

On the other hand, the size of CSNPs plays an important role in their antifungal properties [41]. According to previous studies, CSNPs due to their small size compared with bulk chitosan, which accumulate outside the fungal cells, can diffuse into the fungal cell and disrupt DNA and RNA synthesis. This can explain the more effective antifungal activity of CSNPs compared with chitosan [42]. The difference in CSNPs size obtained from microscopic observations by SEM and DLS analysis in this study could be due to swelling of nanoparticles in aqueous solutions and the formation of hydrogen bonds with H_2O molecules. So, the CSNPs size reported according to SEM image is closer to the real size of CSNPs compared with one analyzed by DLS.

One of the antifungal mechanisms of CSNPs, is the interaction of the surface positive charge of the nanoparticles with the negatively charged phospholipid components of the fungal membrane which leads to an increase in the permeability of the cell membrane, leakage of cell contents, and as a result, fungal cell death [42]. The positive zeta potential of CSNPs is due to protonated amino groups of chitosan. Thus, in addition to the size of CSNPs, zeta potential can also affect the antifungal activity of nanoparticles [40]. By reducing the electrostatic repulsion of CSNPs due to low surface charge, the possibility of nanoparticles accumulation increases [33, 42]. Therefore, in this study, CSNPs with a high positive zeta potential, which indicates the presence of sufficient electrostatic repulsion between nanoparticles and prevents their aggregation, is the reason for the high colloidal stability of CSNPs during sixty days at room temperature without any agglomeration. Based on this, considering the surface absorption of CSNPs by fungal cells as one of the antifungal mechanisms of CSNPs and indicating 1500 ppm as the minimum inhibition concentration of CSNPs against *N. novaehollandiae* in this study, it can be assumed that the existence of high positive charge on the CSNPs surface, not only enables them to interact with the negatively charged components of the fungal membrane, but also increases the chance of this interaction and this can lead to boost CSNPs antifungal properties against *N. novaehollandiae* and its complete inhibition. In addition to size and zeta potential of CSNPs, different fungal species show different responses to the application of CSNPs and fungal species sensitive to CSNPs have a high proportion of phospholipid in their plasma membrane, and previous studies have shown that the higher fluidity of the fungal cell membrane and the higher content of unsaturated fatty acids, could be result to the higher the sensitivity of the fungal species to CSNPs [40]. Therefore, probably the high fluidity of the membrane and the high ratio of phospholipid in the cell membrane of *N. novaehollandiae* could be effective in its sensitivity to CSNPs.

5. Conclusion

In this study, we used CSNPs to inhibit the fungus that causes mulberry canker. In previous studies, the effectiveness of these nanoparticles against other plant pathogens has been proven, and here in, we also proved the antifungal properties of CSNPs against *N. novaehollandiae*. Since the use of chemical fungicides to control plant pathogens has harmful effects on human health and the environment, the use of CSNPs as a suitable alternative is promising. For the future research, investigation the effects of other nanomaterials against *N. novaehollandiae* is suggested.

Funding statement

This research did not receive any specific grant from funding agencies in the public, commercial, or not-for-profit sectors.

Data availability statement

The data that support the findings of this study are available from the corresponding author, [nsafaie@modares.ac.ir], upon reasonable request.

Ethical statement and informed consent

Not applicable.

CRediT authorship contribution statement

Naemeh Mohammadi: Writing – original draft, Visualization, Investigation, Formal analysis, Data curation. **Naser Safaie:** Writing – review & editing, Validation, Supervision, Resources, Project administration, Methodology, Funding acquisition, Formal analysis, Conceptualization. **Maryam Nikkhah:** Validation, Resources, Methodology. **Sajad Moradi:** Validation, Methodology.

Declaration of competing interest

The authors declare that they have no known competing financial interests or personal relationships that could have appeared to influence the work reported in this paper.

Acknowledgments

Gratitude to Tarbiat Modares University for financial support of this project and Melli shimi Keshavarz Company for donating captan fungicide. Also being grateful to Dr. Alizadeh for denoting the causal agent of canker disease in mulberry trees.

References

[1] D. Kb, V. Gv, N.K. Dm, Mulberry as a avenue plant, J. Pharmacogn. Phytochem. 9 (2020) 135–137.
[2] K.S. Dy, P. Wonglom, C. Pornsuriya, A. Sunpapao, Morphological, molecular identification and pathogenicity of Neoscytalidium dimidiatum causing stem canker of Hylocereus polyrhizus in Southern Thailand, Plants 11 (2022) 1–9, https://doi.org/10.3390/plants11040504.
[3] M. Alizadeh, N. Safaie, M. Shams-Bakhsh, M. Mehrabadi, Neoscytalidium novaehollandiae causes dieback on Pinus eldarica and its potential for infection of urban forest trees, Sci. Rep. 12 (2022) 1–15, https://doi.org/10.1038/s41598-022-13414-8.
[4] P. Wonglom, C. Pornsuriya, A. Sunpapao, A new species of Neoscytalidium hylocereum sp. nov. causing canker on red-fleshed dragon fruit (Hylocereus polyrhizus) in Southern Thailand, J. Fungi 9 (2023) 1–12, https://doi.org/10.3390/jof9020197.
[5] E. Oksal, Prevalence molecular characterization and variety reactions of Neoscytalidium novaehollandiae on mulberries in Turkey, J. Not Bot Horti Agrobot Cluj Napoca (2022) 2–13, https://doi.org/10.15835/nbha50212716.
[6] J.D. Ray, T. Burgess, V.M. Lanoiselet, First record of Neoscytalidium dimidiatum and N. novaehollandiae on Mangifera indica and N. dimidiatum on Ficus carica in Australia, Australas, Plant Dis. Notes. 5 (2010) 48–50, https://doi.org/10.1071/DN10018.
[7] M. Sabernasab, S. Jamali, A. Marefat, S. Abbasi, Morphological and molecular characterization of Neoscytalidium novaehollandiae, the cause of Quercus brantii dieback in Iran, Phytopathol. Mediterr. 58 (2019) 347–357, https://doi.org/10.14601/Phytopathol_Mediter-10621.
[8] S. Kurt, A. Uysal, E.M. Soylu, M. Kara, S. Soylu, First record of Neoscytalidium novaehollandiae associated with pistachio dieback in the Southeastern Anatolia region of Turkey, Mycol Iran 6 (2019) 55–57, https://doi.org/10.22043/mi.2020.121015.
[9] D.S. Akgül, N. Savas, M. Özarslandan, First report of wood canker caused by Lasiodiplodia exigua and Neoscytalidium novaehollandiae on grapevine in Turkey, Plant Dis. (2019) 1–2, https://doi.org/10.1094/PDIS-11-18-1938-PDN.
[10] S. Derviş, G. Özer, S. Türkölmez, First report of Neoscytalidium novaehollandiae causing stem blight on tomato in Turkey, J. Plant Pathol. (2020) 1–2, https://doi.org/10.1007/s42161-020-00627-x.
[11] E. Ören, R. Koca, H. Bayraktar, First Report of Neoscytalidium novaehollandiae associated with branch dieback on Japanese Persimmon in Turkey, J. Plant Pathol. (2020) 1–2, https://doi.org/10.1007/s42161-020-00595-2.
[12] E. Ören, G. Koca, R. Gencer, H. Bayraktar, First report of Neoscytalidium novaehollandiae associated with stem canker and branch dieback of almond trees, Australas. Plant Dis. Notes 17 (2020) 1–3, https://doi.org/10.1007/s13314-020-00386-9.
[13] N. Sakci, S. Kurt, A. Uysal, E.M. Soylu, M. Kara, S. Soylu, Identification and pathogenicity of Neoscytalidium novaehollandiae, the agent of canker and dieback in almonds and in vitro activities of some fungicides, Y. Y. U J. Agr Sci. 32 (2022) 132–142, https://doi.org/10.29133/yyutbd.964030.
[14] E. Oksal, G. Özer, First report of shoot blight and branch canker of Pyrus communis by Neoscytalidium novaehollandiae in Turkey, J. Plant Pathol. (2021) 1–2, https://doi.org/10.1007/s42161-021-00762-z.
[15] S. Derviş, İ.G. Güney, İ. Koşar, T. Bozoğlu, G. Özer, First report of Neoscytalidium novaehollandiae on common sage (Salvia officinalis), Australas, Plant Dis. Notes. 19 (2021) 1–4, https://doi.org/10.1007/s13314-021-00433-z.
[16] E. Ören, G. Palacıoğlu, G.N. Ozan, K. Çelik, H. Bayraktar, First report of Neoscytalidium novaehollandiae associated with canker and branch dieback on cherry trees in Turkey, J. Plant Pathol. 104 (2022) 391, https://doi.org/10.1007/s42161-021-00955-6.
[17] E. Ören, G. Palacıoğlu, G.N. Ozan, H. Bayraktar, First Report of Neoscytalidium novaehollandiae associated with branch dieback and stem canker on plum in Turkey, J. Plant Pathol. (2022), https://doi.org/10.1007/s42161-022-01143-w.
[18] Z.A.M. Al-tememe, E.M. Abdulridha, M. Ahmed abbas, A.A. Kareem, The First record of canker fungus Neoscytalidium dimidiatum in Mours alba L. and its diagnosis by using PCR in Karbala, Iraq, J. Plant Arch. 20 (2020) 7971–7975.
[19] S.M. Al-Raish, E.E. Saeed, A. Sham, K. Alblooshi, K.A. El-Tarabily, S.F. AbuQamar, Molecular characterization and disease control of stem canker on royal poinciana (Delonix regia) caused by Neoscytalidium dimidiatum in the United Arab Emirates, Int. J. Sci. 21 (2020) 1–17, https://doi.org/10.3390/ijms21031033.
[20] A.E. Sür, E. Oksal, In vítro efficiency of some fungícídes against Neoscytalídíum dímídíatum (Penz.) Crous and Slippers causing sudden shoot dry on aprícot trees, TURJFAS 9 (2021) 797–802, https://doi.org/10.24925/turjaf.v9i4.797-802.4235.
[21] C. Bragard, P. Baptista, E. Chatzivassiliou, F. Di Serio, P. Gonthier, J.A. Jaques Miret, A.F. Justesen, A. MacLeod, C.S. Magnusson, P. Milonas, Pest categorisation of Neoscytalidium dimidiatum, J. EFSA 21 (2023) 1–56, https://doi.org/10.2903/j.efsa.2023.8001.
[22] N.T. Hieu, N.N.A. Thu, D.T. Linh, N.T.K. Thanh, N.V. Hoa, M. Rangaswamy, Effect of various degree of canopy pruning on plant growth, yield, and control of canker disease of dragon fruit crop, International Conference on Tropical Fruit Pests and Diseases (2018) 98–104.

[23] N. HuiFang, H. ChiaoWen, H. SuiLi, L. SuYu, Y. HongRen, Pathogen characterization and fungicide screening of stem canker of pitaya, J. T. A. R. 62 (2013) 225–234.
[24] Z.A.M. Al-Tememe, A.A. Lahuf, R.G. Abdalmoohsin, A.T. Al-Amirry, Occurrence, identification, pathogenicity and control of Neoscytalidium dimidiatum fungus, the causal agent of sooty canker on Eucalyptus camaldulensis in Karbala Province of Iraq, J. Plant Arch. 19 (2019) 31–38.
[25] J.D. Taguiam, E. Evallo, M.A. Balendres, Reduction of Selenicereus stem cuttings weight by fungal plant pathogens during storage, J. Phytopathol. 169 (2021) 577–580, https://doi.org/10.1111/jph.13024.
[26] N.H. Hoang, T. Le Thanh, R. Sangpueak, J. Treekoon, C. Saengchan, W. Thepbandit, N.K. Papathoti, A. Kamkaew, N. Buensanteai, Chitosan nanoparticles-based ionic gelation method: a promising candidate for plant disease management, Polym. J. 14 (2022) 1–28, https://doi.org/10.3390/polym14040662.
[27] W. Elmer, J.C. White, The future of nanotechnology in plant pathology, Annu. Rev. Phytopathol. 56 (2018) 111–133, https://doi.org/10.1146/annurev-phyto-080417-050108.
[28] A. Kheiri, S.A. Moosawi Jorf, A. Malihipour, H. Saremi, M. Nikkhah, Synthesis and characterization of chitosan nanoparticles and their effect on Fusarium head blight and oxidative activity in wheat, Int. J. Biol. Macromol. 102 (2017) 526–538, https://doi.org/10.1016/j.ijbiomac.2017.04.034.
[29] K. Divya, K. Smitha, M.S. Jisha, Antifungal, antioxidant and cytotoxic activities of chitosan nanoparticles and its use as an edible coating on vegetables, Int. J. Biol. Macromol. 114 (2017) 572–577, https://doi.org/10.1016/j.ijbiomac.2018.03.130.
[30] E. González-Domínguez, G. Fedele, F. Salinari, V. Rossi, A general model for the effect of crop management on plant disease epidemics at different scales of complexity, J. Agron. 10 (2020) 1–23, https://doi.org/10.3390/agronomy10040462.
[31] L.V. Madden, G. Hughes, Plant disease incidence: distributions, heterogeneity, and temporal analysis, Annu. Rev. Phytopathol. 33 (1995) 529–564, https://doi.org/10.1146/annurev.py.33.090195.002525.
[32] B.D. Du, D.T.B. Ngoc, N.D. Thang, L.N.A. Tuan, B.D. Thach, N.Q. Hien, Synthesis and in vitro antifungal efficiency of alginate-stabilized Cu2O-Cu nanoparticles against Neoscytalidium dimidiatum causing brown spot disease on dragon fruit plants (Hylocereus undatus), Vietnam J. Chem. 57 (2019) 318–323, https://doi.org/10.1002/vjch.201900022.
[33] P. Calvo, C. Remunan-Lopez, J.L. Vila-Jato, M.J. Alonso, Novel hydrophilic chitosan–polyethylene oxide nanoparticles as protein carriers, J. Appl. Polym. Sci. 63 (1997) 125–132, https://doi.org/10.1002/(SICI)1097-4628(19970103)63:1%3C125::AIDAPP13%3E3.0.CO.
[34] J.-W. Oh, S.C. Chun, M. Chandrasekaran, Preparation and in vitro characterization of chitosan nanoparticles and their broad-spectrum antifungal action compared to antibacterial activities against phytopathogens of tomato, J. Agron. 9 (2019) 1–12, https://doi.org/10.3390/agronomy9010021.
[35] W. Fan, W. Yanb, Z. Xub, H. Nia, Formation mechanism of monodisperse, low molecular weight chitosan nanoparticles by ionic gelation technique, Colloids Surf., B 90 (2012) 21–27, https://doi.org/10.1016/j.colsurfb.2011.09.042.
[36] A. Nourian, M. Salehi, N. Safaie, F. Khelghatibana, J. Abdollahzadeh, Fungal canker agents in apple production hubs of Iran, Sci. Rep. 11 (2021) 22646, https://doi.org/10.1038/s41598-021-02245-8.
[37] A. Nourian, M. Salehi, N. Safaie, F. Khelghatibana, Biocontrol of Diplodia bulgarica, the causal agent of apple canker, using Trichoderma zelobreve, Arch. Microbiol. 206 (2024) 120, https://doi.org/10.1007/s00203-024-03852-5.
[38] Z. Ranjbar, M. Salehi, N. Safaie, An endophytic Trichoderma-based wettable powder formulation for biocontrol of apple stem cankers, J. Phytopathol. 172 (2024) e13266, https://doi.org/10.1111/jph.13266.
[39] R.A. Hashad, R.A.H. Ishaka, S. Fahmy, S. Mansour, A.S. Geneidi, Chitosan-tripolyphosphate nanoparticles: Optimization of formulation parameters for improving process yield at a novel pH using artificial neural networks, IJBM 86 (2016) 50–58, https://doi.org/10.1016/j.ijbiomac.2016.01.042.
[40] P. Poznanski, A. Hameed W. Orczyk, Chitosan and chitosan nanoparticles: parameters enhancing antifungal activity, J. Mol. 28 (2023) 1–16, https://doi.org/10.3390/molecules28072996.
[41] R. Jha, R.A. Mayanovic, A review of the preparation, characterization, and applications of chitosan nanoparticles in nanomedicine, J. Nanomater. 13 (2023) 1–20, https://doi.org/10.3390/nano13081302.
[42] L.y. Ing, N.m. Zin, A.H. Katas, Antifungal activity of chitosan nanoparticles and correlation with their physical properties, Int. J. Biomater. 2012 (2012), https://doi.org/10.1155/2012/632698.